



Duality, inverse problems and nonlinear problems in solid mechanics

## A homogenization-based constitutive model for two-dimensional viscoplastic porous media

Kostas Danas<sup>a,b,\*</sup>, Martin I. Idiart<sup>a,b</sup>, Pedro Ponte Castañeda<sup>a,b</sup>

<sup>a</sup> *Laboratoire de mécanique des solides, CNRS UMR7649, département de mécanique, École polytechnique, 91128 Palaiseau cedex, France*

<sup>b</sup> *Department of Mechanical Engineering and Applied Mechanics, University of Pennsylvania, Philadelphia, PA 19104-6315, USA*

### Abstract

An approximate model based on the so-called ‘second-order’ nonlinear homogenization method is proposed to estimate the effective behavior of viscoplastic porous materials exhibiting transversely isotropic symmetry. The model is constructed in such a way that it reproduces exactly the behavior of a ‘composite-cylinder assemblage’ in the limit of in-plane hydrostatic loading, and therefore coincides with the hydrostatic limit of Gurson’s criterion for plastic porous materials. As a consequence, the new model improves on earlier ‘second-order’ homogenization estimates, which have been found to be overly stiff at sufficiently high triaxialities and nonlinearities. The proposed model is compared with exact results obtained for a special class of porous materials with sequentially laminated microstructures. The agreement is found to be excellent for the entire range of stress triaxialities, and all values of the porosity and nonlinearity considered. *To cite this article: K. Danas et al., C. R. Mecanique 336 (2008).*

© 2007 Académie des sciences. Published by Elsevier Masson SAS. All rights reserved.

### Résumé

**Un modèle d’homogénéisation pour les matériaux poreux viscoplastiques bi-dimensionnels.** On propose un modèle approximatif fondé sur la méthode d’homogénéisation non-linéaire dite du « second-ordre » pour estimer le comportement effectif des matériaux poreux viscoplastiques isotropes transverses. Le modèle est construit de manière à reproduire exactement le comportement hydrostatique des « assemblages de cylindres composites », c’est-à-dire la limite hydrostatique des matériaux poreux plastiques fournis par le critère de Gurson. Par conséquent, le nouveau modèle améliore les estimations de « second-ordre » existantes, qui se sont avérées excessivement raides aux triaxialités et aux non-linéarités suffisamment élevées. Le modèle proposé est comparé aux résultats exacts obtenus pour une classe particulière de matériaux poreux présentant des microstructures séquentiellement stratifiées. L’accord s’avère excellent pour la gamme entière des triaxialités, ainsi que pour toutes les valeurs de la porosité et de l’exposant caractérisant la non-linéarité du comportement. *Pour citer cet article : K. Danas et al., C. R. Mecanique 336 (2008).*

© 2007 Académie des sciences. Published by Elsevier Masson SAS. All rights reserved.

**Keywords:** Porous media; Homogenization; Nonlinear composites; Gurson criterion

**Mots-clés :** Milieux poreux ; Homogénéisation ; Composites non-linéaires ; Critère de Gurson

\* Corresponding author.

*E-mail addresses:* [kdanas@seas.upenn.edu](mailto:kdanas@seas.upenn.edu) (K. Danas), [midiart@seas.upenn.edu](mailto:midiart@seas.upenn.edu) (M.I. Idiart), [ponte@seas.upenn.edu](mailto:ponte@seas.upenn.edu) (P. Ponte Castañeda).

## 1. Introduction

The modeling of void growth and ductile damage of viscoplastic composites has been the subject of numerous works over the past forty years. Various models have been proposed for the estimation of the effective behavior of isotropic porous materials starting with the Gurson model [1]. Gurson made use of the exact solution for a shell (spherical or cylindrical cavity) subjected to hydrostatic loading, together with a uniform, purely deviatoric field, to obtain estimates for the effective behavior of rigid-perfectly plastic, porous solids. About fifteen years earlier than Gurson, Hashin [2] proposed an exact solution for the effective behavior of a special class of linear-elastic composites known as the composite-sphere assemblage (CSA), and composite-cylinder assemblage (CCA), when subjected to hydrostatic loading. Leblond et al. [3] generalized these results for nonlinear porous media and proposed approximate models for porous viscoplastic composites, with cylindrical and spherical microstructures.

In a separate development, Ponte Castañeda [4] (see also Willis [5] and Michel and Suquet [6]) obtained rigorous bounds of the Hashin–Shtrikman type [7] for porous nonlinear materials by making use—via a suitably designed variational principle—of an optimally chosen ‘linear comparison composite’ with the same microstructure as the nonlinear composite. Generalizing the notion of an optimally selected linear comparison composite to more general types of comparison materials (anisotropic thermoelastic phases), Ponte Castañeda [8] proposed the ‘second-order’ method, which improved on the earlier ‘variational’ method by accounting for the anisotropic distribution of the local fields in nonlinear media, and obtained more accurate estimates for the effective behavior of isotropic porous nonlinear media [9]. However, these estimates have been found to be too ‘stiff’ at sufficiently high triaxialities and nonlinearities [10]. Even though, the interest in this work is for small porosities, the above methods may also be applied to composites with high porosities, where they are much more accurate. In this context, Despois et al. [11] have used the variational estimate to compare with experimental data for metal foams.

Following deBotton and Ponte Castañeda [12], deBotton and Hariton [13] obtained exact results for a special class of two-phase nonlinear composites with sequentially laminated random microstructures and isotropic, incompressible phases. Their analysis can be generalized to the case of compressible phases [14], so that exact results for porous sequential laminates can be obtained. In the context of the present work, the interest in porous materials with this special type of microstructure stems from the fact that, in the linear case, their effective behavior can be shown (e.g., [15,16]) to agree exactly with the Hashin–Shtrikman estimates, for any choice of the modulus tensors of the phases. As will become evident later, sequential laminates are particularly appropriate for assessing the accuracy of the aforementioned linear comparison methods.

The purpose of this work is to improve the high-triaxiality behavior of the second-order model for nonlinear porous materials, and to compare the resulting estimates to (numerically) exact solutions for materials with sequentially laminated microstructures, for the full range of triaxiality. Although in this work we will only consider porous power-law materials with cylindrical pores (and transversely isotropic macroscopic behavior) subjected to plane-strain loading, the ideas are general and can be used for more general types of porous materials, including fully isotropic materials subjected to three-dimensional loading. The objective here is to test the basic ideas of the improved second-order model in the context of the simplest possible non-trivial case.

We consider a representative volume element  $\Omega$  of a two-phase porous medium with each phase occupying a subdomain  $\Omega^{(r)}$  ( $r = 1, 2$ ). The vacuum phase is identified as phase 2, while the non-vacuum phase (i.e., matrix phase) is denoted as phase 1. The local behavior of the matrix phase is characterized by a convex isotropic stress potential, such that the Cauchy stress  $\boldsymbol{\sigma}$  and the Eulerian strain-rate  $\mathbf{D}$  at any point in  $\Omega^{(1)}$  are related by

$$\mathbf{D} = \frac{\partial U^{(1)}}{\partial \boldsymbol{\sigma}}(\boldsymbol{\sigma}), \quad \text{with } U^{(1)}(\boldsymbol{\sigma}) = \frac{\sigma_o}{n+1} \left( \frac{\sigma_{\text{eq}}}{\sigma_o} \right)^{n+1} \quad (1)$$

Here, the von Mises stress is defined in terms of the deviatoric stress tensor as  $\sigma_{\text{eq}} = \sqrt{\frac{3}{2} \boldsymbol{\sigma}_d \cdot \boldsymbol{\sigma}_d}$ ,  $\sigma_o$  denotes the flow stress of the matrix phase, and  $m = 1/n$  is the strain-rate sensitivity parameter, which takes values between 0 and 1. Note that the two limiting values  $m = 1$  and  $m = 0$  correspond to linear and rigid-perfectly plastic behaviors, respectively.

The effective behavior of the porous material is defined as the relation between the average stress,  $\bar{\boldsymbol{\sigma}} = \langle \boldsymbol{\sigma} \rangle$ , and the average strain-rate,  $\bar{\mathbf{D}} = \langle \mathbf{D} \rangle$ , which can also be characterized by an effective stress potential  $\tilde{U}$ , such that [17]

$$\bar{\mathbf{D}} = \frac{\partial \tilde{U}}{\partial \bar{\boldsymbol{\sigma}}}, \quad \tilde{U}(\bar{\boldsymbol{\sigma}}) = (1-f) \inf_{\boldsymbol{\sigma} \in \mathcal{S}(\bar{\boldsymbol{\sigma}})} \langle U^{(1)}(\boldsymbol{\sigma}) \rangle^{(1)} \quad (2)$$

Here,  $\langle \cdot \rangle$  and  $\langle \cdot \rangle^{(r)}$  denote the volume averages over the representative volume element  $\Omega$  and over the sub-domains  $\Omega^{(r)}$  ( $r = 1, 2$ ), respectively,  $f$  denotes the volume fraction of the porous phase (i.e., the porosity), and  $\mathcal{S}(\bar{\sigma}) = \{\sigma, \text{div } \sigma = 0 \text{ in } \Omega, \sigma \mathbf{n} = \mathbf{0} \text{ on } \partial\Omega^{(2)}, \langle \sigma \rangle = \bar{\sigma}\}$  is the set of statically admissible stresses.

In the present work, the focus is on porous materials containing cylindrical voids aligned with the  $x_3$ -axis, which are randomly and isotropically distributed in the transverse plane  $x_1$ - $x_2$ . The material is subjected to plane-strain loadings, so that  $\bar{D}_{i3} = 0$  with  $i = 1, 2, 3$ .

From the homogeneity of the local potential (1)<sub>2</sub> in  $\sigma$ , it follows that the effective potential (2) is a homogeneous function of degree  $n + 1$  in  $\bar{\sigma}$ . It is then convenient to introduce the so-called gauge factor  $\Lambda$ , such that [3]

$$\tilde{U}(\bar{\sigma}) = \frac{\sigma_o}{n+1} \left( \frac{\Lambda(\bar{\sigma}; f)}{\sigma_o} \right)^{n+1} \tag{3}$$

which, in turn, allows us to define the gauge function via

$$\Phi_n(\bar{\Sigma}) = \tilde{U}(\bar{\Sigma}) - \frac{\sigma_o^{-n}}{n+1} = 0, \quad \text{with } \bar{\Sigma} = \frac{\bar{\sigma}}{\Lambda(\bar{\sigma}; f)} \tag{4}$$

This gauge function is a suitably normalized quantity that is homogeneous of degree zero in the stress  $\bar{\sigma}$ . It is also convenient to introduce the normalized, macroscopic strain-rate

$$\bar{E} = \frac{\bar{D}}{(\Lambda(\bar{\sigma}; f)/\sigma_o)^n} = \frac{\partial \Lambda(\bar{\sigma}; f)}{\partial \bar{\sigma}} \tag{5}$$

and the macroscopic stress and strain-rate triaxialities

$$X_\Sigma = \frac{\bar{\Sigma}_m}{\bar{\Sigma}_{\text{eq}}} = \frac{\bar{\sigma}_m}{\bar{\sigma}_{\text{eq}}} \quad \text{and} \quad X_E = \frac{\bar{E}_m}{\bar{E}_{\text{eq}}} = \frac{\bar{D}_m}{\bar{D}_{\text{eq}}} \tag{6}$$

where the normalized, in-plane mean stress and strain-rate are defined as  $\bar{\Sigma}_m = (\bar{\Sigma}_{11} + \bar{\Sigma}_{22})/2$ ,  $\bar{E}_m = (\bar{E}_{11} + \bar{E}_{22})/2$ , and  $\bar{\Sigma}_{\text{eq}}$  and  $\bar{E}_{\text{eq}}$  denote the von Mises equivalent parts of the normalized stress and strain-rate, respectively.

Thus, the problem of estimating the effective behavior of the porous material is equivalent to that of estimating the function  $\tilde{U}$  in relation (2)<sub>2</sub>. However, computing this function exactly is an extremely difficult task, in general. In the next section, a method for estimating this function is recalled and applied to the class of porous materials of interest in this work.

## 2. Second-order variational estimates

To estimate the effective stress potential  $\tilde{U}$ , the second-order method, originally proposed by Ponte Castañeda [8], is described next. The method is based on the construction of a “*linear comparison composite*” (*LCC*), with the same microstructure as the nonlinear composite, whose constituent phases are identified with appropriate linearizations of the given nonlinear phases resulting from a suitably designed variational principle. This allows the use of any method already available to estimate the effective behavior of *linear* composites to generate corresponding estimates for *nonlinear* composites.

For the class of materials considered in this work, the *LCC* is a porous material, with a matrix phase characterized by

$$U_L(\sigma; \check{\sigma}, \mathbf{M}) = U(\check{\sigma}) + \frac{\partial U}{\partial \sigma}(\check{\sigma}) \cdot (\sigma - \check{\sigma}) + \frac{1}{2}(\sigma - \check{\sigma}) \cdot \mathbf{M}(\sigma - \check{\sigma}) \tag{7}$$

where the label ‘1’ (denoting the matrix phase) will be omitted for simplicity in the rest of the section. In this expression, the tensor  $\check{\sigma}$  is a uniform reference stress tensor to be defined later, and  $\mathbf{M}$  is a symmetric, fourth-order, compliance tensor of the form [8]

$$\mathbf{M} = \frac{1}{2\lambda} \mathbf{E} + \frac{1}{2\mu} \mathbf{F}, \quad \text{with } \mathbf{E} = \frac{3}{2} \frac{\check{\sigma}_d \otimes \check{\sigma}_d}{\check{\sigma}_{\text{eq}}^2}, \quad \mathbf{F} = \mathbf{K} - \mathbf{E} \tag{8}$$

In this last expression,  $\mathbf{K}$  denotes the in-plane components of the standard, fourth-order, isotropic, shear projection tensor, whereas the subscript  $d$  denotes the deviatoric part of  $\check{\sigma}$ . The quantities  $\mathbf{E}$  and  $\mathbf{F}$  correspond to the fourth-order eigen-tensors of the tangent compliance tensor [18], defined by  $\mathbf{M}_t = \frac{\partial^2 U}{\partial \sigma \partial \sigma}(\check{\sigma})$ , and they are such that  $\mathbf{E}\mathbf{E} =$

$\mathbf{E}$ ,  $\mathbf{F}\mathbf{F} = \mathbf{F}$ ,  $\mathbf{E}\mathbf{F} = \mathbf{0}$ . It is emphasized that, even though the nonlinear matrix phase is *isotropic* (see relation (1)), the corresponding linearized phase in the *LCC* is, in general, *anisotropic*, in contrast with earlier methods, like the variational method introduced by Ponte Castañeda [4], where the corresponding *LCC* is isotropic. A measure of this anisotropy is given by the ratio  $k = \lambda/\mu$ , such that  $k = 1$  and  $k = 0$  correspond to an isotropic and extremely anisotropic linear matrix phase. Once the linear comparison composite is defined, then linear homogenization theories, such as the Hashin–Shtrikman theory [7], may be used to deliver estimates for the effective behavior of the *LCC*, which in turn can be used to generate corresponding estimates for the nonlinear composite.

Making use of an appropriate specialization of the Levin [19] relations for two-phase thermoelastic materials, the effective potential of the *LCC* can be written as

$$\tilde{U}_L(\bar{\boldsymbol{\sigma}}; \check{\boldsymbol{\sigma}}, \mathbf{M}) = (1-f)U(\check{\boldsymbol{\sigma}}) + \boldsymbol{\eta} \cdot (\bar{\boldsymbol{\sigma}} - (1-f)\check{\boldsymbol{\sigma}}) + \frac{1}{2}\bar{\boldsymbol{\sigma}} \cdot \tilde{\mathbf{M}}\bar{\boldsymbol{\sigma}} - \frac{1-f}{2}\check{\boldsymbol{\sigma}} \cdot \mathbf{M}\check{\boldsymbol{\sigma}} \quad (9)$$

where  $\boldsymbol{\eta} = \partial U/\partial \check{\boldsymbol{\sigma}} - \mathbf{M}\check{\boldsymbol{\sigma}}$ , and  $\tilde{\mathbf{M}}$  denotes the effective compliance tensor of the *LCC*. Thus, expression (9) requires an estimate for  $\tilde{\mathbf{M}}$ . In this work, use is made of the generalized Hashin–Shtrikman estimates of Willis [20], which are known to be quite accurate for particulate random systems like the ones of interest in this work, up to moderate concentrations of inclusions. For porous materials, these estimates take the form

$$\tilde{\mathbf{M}} = \frac{1}{1-f}\mathbf{M} + \frac{f}{1-f}(\mathbf{P}^{-1} - \mathbf{M}^{-1})^{-1} \quad (10)$$

Here,  $\mathbf{P}$  is a microstructural tensor, related to the Eshelby tensor [21], which depends on  $\mathbf{M}$  and requires, in general, the numerical evaluation of certain integrals. However, for the case of interest here, the tensor  $\mathbf{P}$  is such that [9]

$$(\mathbf{P}^{-1} - \mathbf{M}^{-1})^{-1} = \frac{1}{2\sqrt{\lambda\mu}}\mathbf{I} = \frac{1}{2\sqrt{\lambda\mu}}(\mathbf{K} + \mathbf{J}) \quad (11)$$

with  $\mathbf{I}$  and  $\mathbf{J}$  denoting the in-plane components of the standard, fourth-order, symmetric, identity and hydrostatic projection tensor, respectively. In the last relation, the relevant hydrostatic components associated with the hydrostatic projection tensor  $\mathbf{J}$ , imply that the effective behavior of the corresponding *LCC* (i.e., in relation (9)) is compressible. Thus, expressions (9)–(11) completely characterize the *LCC* in terms of the reference tensor  $\check{\boldsymbol{\sigma}}$  and the matrix compliance  $\mathbf{M}$ .

Then, the ‘second-order’ estimate for the effective stress potential of the nonlinear porous material is given by [8]

$$\tilde{U}_{SOM}(\bar{\boldsymbol{\sigma}}) = \text{stat}_{\lambda, \mu} \{ \tilde{U}_L(\bar{\boldsymbol{\sigma}}; \check{\boldsymbol{\sigma}}, \mathbf{M}) + (1-f)V(\check{\boldsymbol{\sigma}}, \mathbf{M}) \} \quad (12)$$

where  $\tilde{U}_L$  is given by (9), and the ‘corrector’ function  $V$  is defined as

$$V(\check{\boldsymbol{\sigma}}, \mathbf{M}) = \text{stat}_{\check{\boldsymbol{\sigma}}} [U(\hat{\boldsymbol{\sigma}}) - U_L(\hat{\boldsymbol{\sigma}}; \check{\boldsymbol{\sigma}}, \mathbf{M})] \quad (13)$$

In these expressions, the stationary operation (stat) consists in setting the partial derivative of the argument with respect to the variable equal to zero, which yields a set of nonlinear equations for the variables  $\lambda$ ,  $\mu$  and  $\hat{\boldsymbol{\sigma}}$ , as shown next.

Making use of the special form of the tensor  $\mathbf{M}$ , we can define two components of the tensor  $\hat{\boldsymbol{\sigma}}$  that are parallel and perpendicular to the corresponding reference tensor  $\check{\boldsymbol{\sigma}}$ , respectively,  $\hat{\boldsymbol{\sigma}}_{\parallel} = (\frac{3}{2}\hat{\boldsymbol{\sigma}} \cdot \mathbf{E}\hat{\boldsymbol{\sigma}})^{1/2}$  and  $\hat{\boldsymbol{\sigma}}_{\perp} = (\frac{3}{2}\hat{\boldsymbol{\sigma}} \cdot \mathbf{F}\hat{\boldsymbol{\sigma}})^{1/2}$ , such that the equivalent part of the tensor  $\hat{\boldsymbol{\sigma}}$  reduces to  $\hat{\boldsymbol{\sigma}}_{\text{eq}} = \sqrt{\hat{\boldsymbol{\sigma}}_{\parallel}^2 + \hat{\boldsymbol{\sigma}}_{\perp}^2}$ . The stationarity operation in (13) then leads to two equations which can be combined to obtain the relation

$$k \left( \frac{\hat{\boldsymbol{\sigma}}_{\text{eq}}}{\check{\boldsymbol{\sigma}}_{\text{eq}}} \right)^{1-n} = (k-1) \frac{\hat{\boldsymbol{\sigma}}_{\parallel}}{\check{\boldsymbol{\sigma}}_{\text{eq}}} + 1 \quad (14)$$

The scalar quantities  $\hat{\boldsymbol{\sigma}}_{\text{eq}}$  and  $\hat{\boldsymbol{\sigma}}_{\parallel}$  are functions of the applied macroscopic loading  $\bar{\boldsymbol{\sigma}}$ , the material properties and the microstructure, and result from the stationarity condition in relation (12) with respect to  $\lambda$  and  $\mu$ , such that [22]

$$\begin{aligned} \hat{\boldsymbol{\sigma}}_{\parallel} - \check{\boldsymbol{\sigma}}_{\text{eq}} &= \sqrt{\frac{3}{1-f} \frac{\partial \tilde{U}_L}{\partial (2\lambda)^{-1}}} = \sqrt{\frac{3}{1-f} \langle (\boldsymbol{\sigma}_L - \check{\boldsymbol{\sigma}}) \cdot \mathbf{E}(\boldsymbol{\sigma}_L - \check{\boldsymbol{\sigma}}) \rangle^{(1)}} \\ \hat{\boldsymbol{\sigma}}_{\perp} &= \sqrt{\frac{3}{1-f} \frac{\partial \tilde{U}_L}{\partial (2\mu)^{-1}}} = \sqrt{\frac{3}{1-f} \langle \boldsymbol{\sigma}_L \cdot \mathbf{F}\boldsymbol{\sigma}_L \rangle^{(1)}} \end{aligned} \quad (15)$$

where the right-hand sides of these relations depend on certain traces of the field fluctuations in the *LCC*, and  $\sigma_L$  denotes the local stress field in the *LCC*. It should be noted that the right-hand side of the last two equations are homogeneous functions of degree zero in  $\mathbf{M}$ , and therefore, the quantities  $\hat{\sigma}_{\parallel}$  and  $\hat{\sigma}_{\perp}$  depend on the moduli  $\lambda$  and  $\mu$  only through the anisotropy ratio  $k$ . Thus, introducing these expressions for  $\hat{\sigma}_{\parallel}$  and  $\hat{\sigma}_{\perp}$  into (14) we obtain a single algebraic, nonlinear equation for  $k$ , which must be solved numerically, in general, for a given choice of the reference tensor  $\check{\sigma}$ . The evaluation of the two moduli, then, follows simply by noting that  $\mu = (\sigma_o^{-n}/3)\hat{\sigma}_{\text{eq}}^{1-n}$  and  $\lambda = k\mu$ .

Finally, taking into account the two stationarity operations described previously in relations (14) and (15), the expression (12) for the effective stress potential of the nonlinear porous composite can be further simplified to

$$\tilde{U}_{SOM}(\bar{\sigma}) = (1 - f) \left[ \frac{\sigma_o}{1+n} \left( \frac{\hat{\sigma}_{\text{eq}}}{\sigma_o} \right)^{n+1} - \left( \frac{\check{\sigma}_{\text{eq}}}{\sigma_o} \right)^n \left( \hat{\sigma}_{\parallel} - \frac{\bar{\sigma}_{\text{eq}}}{(1-f)} \right) \right] \quad (16)$$

where the tensor  $\check{\sigma}$  still remains to be defined.

It should be emphasized at this point that the ‘second-order’ estimate (12) involves *two* approximations: the *homogenization* of the *LCC* and the *linearization* of the nonlinear composite. The first one is associated with the estimation of the effective behavior of the *LCC* by making use of the Willis estimates (see relations (7)–(11)), which are expected to be sufficiently good for low to moderate porosities. The second approximation lies in the construction and optimization of the *LCC*, as described in relations (12)–(16).

The corresponding macroscopic stress-strain-rate relation follows from differentiation of (12) or, equivalently, (16). In the present case, the resulting expression can be shown to reduce to [23]

$$\bar{\mathbf{D}} = \bar{\mathbf{D}}_L + (1 - f) \left( \frac{\partial \check{\sigma}}{\partial \bar{\sigma}} \right)^T \mathbf{g} \quad (17)$$

where  $\bar{\mathbf{D}}_L = \tilde{\mathbf{M}} \bar{\sigma} + \boldsymbol{\eta}$  is the macroscopic strain-rate of the *LCC*, and the second-order tensor  $\mathbf{g}$  is given by

$$\mathbf{g} = \left( \frac{1}{2\lambda} - \frac{1}{2\lambda_t} \right) \left( \hat{\sigma}_{\parallel} - \frac{\bar{\sigma}_{\text{eq}}}{(1-f)} \right) \frac{\check{\sigma}}{\check{\sigma}_{\text{eq}}}, \quad \text{with } \lambda_t = \frac{\sigma_o}{3n} \left( \frac{\check{\sigma}_{\text{eq}}}{\sigma_o} \right)^{1-n} \quad (18)$$

### 2.1. Choices for the reference stress tensor

The estimate (16) requires a prescription for the reference stress tensor  $\check{\sigma}$ . In this section, a prescription suitable for the class of porous materials considered in this work is proposed. As already discussed in previous works ([8,24]), it has not yet been possible to optimize the choice of the reference stress tensor. Nonetheless, it is still possible to propose physically motivated choices for the reference stress tensor, that in turn, satisfy certain special properties to be made explicit in the following discussion. Here, we restrict our attention to the specific problem described in the beginning of the section, but before proceeding to specific propositions for the reference stress tensor, it is worth recalling first some basic results that will prove helpful in the discussion below.

It is well known that, when an aggregate of an infinite hierarchy of sizes of cylindrical shells, called the composite cylinder-assembly (*CCA*) of Hashin [2], is subjected to hydrostatic conditions (i.e.,  $|X_{\Sigma}| \rightarrow \infty$ ), the last admits an exact solution [3]. The effective behavior of such a composite is obtained by solving the isolated shell problem, and is given by

$$\tilde{U}_{\text{shell}}(\bar{\sigma}_m) = \frac{\tilde{\sigma}_H}{1+n} \left( \frac{\bar{\sigma}_m}{\tilde{\sigma}_H} \right)^{1+n}, \quad \text{with } \frac{\tilde{\sigma}_H}{\sigma_o} = \frac{1}{m} \left( \frac{1}{f^m} - 1 \right) \frac{1}{3^{(1+m)/2}} \quad (19)$$

Here,  $\tilde{\sigma}_H$  is the effective flow stress of the shell, which is a function of the porosity  $f$  and the strain-rate sensitivity parameter of the matrix  $m$ . On the other hand, the effective flow stress delivered by the variational procedure of Ponte Castañeda [4] (*VAR*), in the special case of pure hydrostatic loading, reduces to

$$\frac{\tilde{\sigma}_{HVAR}}{\sigma_o} = (1 - f) \left( \frac{1}{3f} \right)^{(1+m)/2} \quad (20)$$

which clearly deviates from the exact solution (19) for values of  $m$  different from 1 (i.e., the linear case), particularly for small porosities.

Now, in the context of the second-order method, Ponte Castañeda [9] proposed the choice  $\check{\sigma} = \bar{\sigma}_d^{(1)} = \bar{\sigma}_d / (1 - f)$  for the reference stress tensor, where the subscript  $d$  denotes the deviatoric part of a second-order tensor. Unfortunately, this reference tensor tends to zero as the stress triaxiality tends to infinity, and consequently, in the hydrostatic limit, the resulting effective flow stress of this estimate is identical to the one obtained by the variational method (i.e., in relation (20)). In addition, Idiart et al. [22] proposed the following simple choice for the reference stress tensor

$$\check{\sigma} = \bar{\sigma}_d \quad (21)$$

This choice has been shown to deliver reasonably good estimates when the porous composite is subjected to isochoric loadings (i.e.,  $X_\Sigma = 0$ ), but like the aforementioned choice of  $\check{\sigma} = \bar{\sigma}_d^{(1)}$ , it also becomes zero for the case of hydrostatic loading, and thus it leads to the variational estimate (20).

Motivated by these observations, we propose the following ad-hoc choice for the reference stress tensor, which reads as

$$\check{\sigma} = \xi(X_\Sigma) \bar{\sigma}_d, \quad \xi(X_\Sigma) = \frac{1 - tf}{1 - f} + \alpha_m \sqrt{X_\Sigma^2} (\exp[-\alpha_{eq} / \sqrt{X_\Sigma^2}] + \beta \exp[-1 / X_\Sigma^2]) \quad (22)$$

with  $t$  and  $\beta$  being empirical coefficients that ensure the convexity of the gauge function at dilute concentrations and are detailed in Appendix A. The coefficients  $\alpha_m$  and  $\alpha_{eq}$  are, in general, functions of the microstructure, the nonlinearity  $m$  of the matrix, but not of the loading and the stress triaxiality. Before discussing the estimation of the coefficients  $\alpha_m$  and  $\alpha_{eq}$ , it is essential to note that the choice (22) reduces to the choice (21) for  $X_\Sigma = 0$ , while it remains non-zero in the hydrostatic limit  $|X_\Sigma| \rightarrow \infty$ , unlike choice (21) which becomes zero. It also guarantees that the effective stress potential is a homogeneous function of degree  $n + 1$  in the average stress  $\bar{\sigma}$  for all triaxialities  $X_\Sigma \in (-\infty, +\infty)$ . In particular, the coefficient  $\alpha_m$  is computed such that the estimate for the effective stress potential  $\tilde{U}$  coincides with the analytical solution for  $\tilde{U}_{shell}$  in relation (19) in the hydrostatic limit. This condition may be written as

$$\tilde{U}_{SOM} \rightarrow \tilde{U}_{shell} \quad \text{as } |X_\Sigma| \rightarrow \infty \quad \Rightarrow \quad \alpha_m = \alpha_m(m, f) \quad (23)$$

In addition to the analytical estimate (19) for the effective stress potential, the solution of the shell problem also requires that the macroscopic deviatoric strain-rate be zero under purely hydrostatic loads. This condition in turn provides an equation for the estimation of the coefficient  $\alpha_{eq}$ , which can be written as

$$\left( \frac{\partial \tilde{U}_{SOM}}{\partial \bar{\sigma}} \right)_{eq} \rightarrow \left( \frac{\partial \tilde{U}_{shell}}{\partial \bar{\sigma}} \right)_{eq} \quad \Rightarrow \quad \bar{D}_{eq} \rightarrow 0 \quad \text{as } |X_\Sigma| \rightarrow \infty \quad \Rightarrow \quad \alpha_{eq} = \alpha_{eq}(m, f) \quad (24)$$

The computation of the coefficient  $\alpha_m$  needs to be performed numerically, while the expression for  $\alpha_{eq}$  can be further simplified to the analytical expression

$$\alpha_{eq} = \alpha_m^{-1} \left( 1 + \frac{\frac{3}{2} (\check{\sigma}_{eq} / \sigma_o)^n - \check{\sigma}_{eq} (2\lambda)^{-1}}{(1 - f) \hat{\sigma}_\parallel} \left( \frac{1}{2\lambda} - \frac{1}{2\lambda_t} \right)^{-1} \right) \quad (25)$$

where all the quantities involved in the last relation are evaluated in the hydrostatic limit  $|X_\Sigma| \rightarrow \infty$ , and  $\lambda_t$  is given by relation (18)<sub>2</sub>. In summary, relation (22), together with relations (23), (24) and (25), completely define the reference stress tensor  $\check{\sigma}$ , and thus, relation (16) can be used to estimate the effective behavior of the porous material of interest in this work.

For the special case of ideal plasticity ( $m = 0$ ), relation (19) reduces to

$$\frac{\tilde{\sigma}_H}{\sigma_o} = \frac{1}{\sqrt{3}} \ln \left( \frac{1}{f} \right) \quad (26)$$

and  $\alpha_m$  can be determined explicitly (see Appendix B). On the other hand, the equation describing the effective yield surface, predicted by the second-order method, simplifies to

$$\Phi_\infty(\bar{\Sigma}) = \hat{\sigma}_{eq} - \sigma_o = \sqrt{\hat{\sigma}_\parallel^2 + \hat{\sigma}_\perp^2} - \sigma_o = 0 \quad (27)$$

where  $\hat{\sigma}_\parallel$  and  $\hat{\sigma}_\perp$  are defined in relation (15). In the context of these results for the special case of ideally plastic porous materials, it is important to emphasize that we have assumed here that expressions (24) and (25) continue to hold for the determination of  $\alpha_{eq}$ . This is done for simplicity, in spite of existing evidence [10] suggesting that the yield surface of ideally plastic porous materials may exhibit a corner on the hydrostatic axis and, consequently,  $\bar{D}$  may not be uniquely determined at that point (but see also [25]).

### 3. Exact results for porous materials with sequentially laminated microstructures

While the effective stress potential  $\tilde{U}$  cannot be computed exactly, in general, it can be determined for a very special class of composites called ‘sequential laminates’. A sequential laminate is an iterative construction obtained by layering laminated materials (which in turn have been obtained from lower-order lamination procedures) with other laminated materials, or directly with the homogeneous phases that make up the composite, in such a way as to produce hierarchical microstructures of increasing complexity (e.g., [16]). The *rank* of the laminate refers to the number of layering operations required to reach the final sequential laminate. Of the many possible types of sequential laminates, we restrict attention to porous sequential laminates formed by layering at every step a porous laminate with the matrix phase (denoted as phase 1).

Thus, a rank-1 laminate corresponds to a simple laminate with a given layering direction  $\mathbf{n}^{(1)}$ , with matrix and porous phases in proportions  $1 - f_1$  and  $f_1$ . In turn, a rank-2 laminate is constructed by layering the rank-1 laminate with the matrix phase, in a different layering direction  $\mathbf{n}^{(2)}$ , in proportions  $f_2$  and  $1 - f_2$ , respectively. Rank- $M$  laminates are obtained by iterating this procedure  $M$  times, layering the rank- $(M - 1)$  laminate with the matrix phase in the direction  $\mathbf{n}^{(M)}$ , in proportions  $f_M$  and  $1 - f_M$ , respectively. It should be mentioned that in this procedure, it is assumed that the length scale of the embedded laminate is much smaller than the length scale of the embedding laminate. This assumption allows to regard the rank- $(M - 1)$  laminate in the rank- $M$  laminate as a homogeneous phase, so that available expressions for the effective potential of simple laminates (e.g., [12]) can be used at each step of the process to obtain an exact expression for the effective potential of the rank- $M$  sequential laminate (e.g., [26,13]). From their construction process, it follows that the microstructure of these sequential laminates can be regarded as *random* and *particulate*, with phase 1 playing the role of the (continuous) matrix phase embedding the (discontinuous) porous phase. A distinctive feature of this very special class of porous materials is that the strain-rate and stress fields are uniform in the inclusion phase (in this case, the pores) but non-uniform in the matrix phase.

Because the interest here is on porous materials exhibiting overall transverse isotropy, the layering directions  $\mathbf{n}^{(i)}$  ( $i = 1, \dots, M$ ) will be taken to lie on the plane with normal  $\mathbf{e}_3$ . Let  $\mathbf{m}^{(i)}$  ( $i = 1, \dots, M$ ) denote unit vectors orthogonal to  $\mathbf{e}_3$  and the corresponding  $\mathbf{n}^{(i)}$ . Then, it can be shown that the effective stress potential of the resulting rank- $M$  porous laminate may be written as [13,14]

$$\tilde{U}_M(\bar{\boldsymbol{\sigma}}) = \min_{\substack{w^{(i)} \\ \bar{\boldsymbol{\sigma}}^{(2)} = \mathbf{0}}} \sum_{i=1}^M (1 - f_i) \left( \prod_{j=i+1}^M f_j \right) U^{(1)}(\bar{\boldsymbol{\sigma}}_i^{(1)}) \tag{28}$$

where the stress tensors  $\bar{\boldsymbol{\sigma}}_i^{(1)}$  ( $i = 1, \dots, M$ ) and  $\bar{\boldsymbol{\sigma}}^{(2)}$  are given in terms of the optimization variables  $w^{(i)}$  by

$$\bar{\boldsymbol{\sigma}}_i^{(1)} = \bar{\boldsymbol{\sigma}} + f_i w^{(i)} \mathbf{m}^{(i)} \otimes \mathbf{m}^{(i)} - \sum_{j=i+1}^M (1 - f_j) w^{(j)} \mathbf{m}^{(j)} \otimes \mathbf{m}^{(j)}, \quad i = 1, \dots, M \tag{29}$$

$$\bar{\boldsymbol{\sigma}}^{(2)} = \bar{\boldsymbol{\sigma}} - \sum_{i=1}^M (1 - f_i) w^{(i)} \mathbf{m}^{(i)} \otimes \mathbf{m}^{(i)} \tag{30}$$

The total porosity in this rank- $M$  laminate is given by

$$f = \prod_{i=1}^M f_i \tag{31}$$

Thus, expression (28) requires the solution of an  $M$ -dimensional convex minimization problem, which must be solved numerically for a given macroscopic stress  $\bar{\boldsymbol{\sigma}}$ . This minimization problem is constrained by the fact that the (uniform) stress in the porous phase (denoted as phase 2) must be zero. It is noted that this constraint (in the variables  $w^{(i)}$ ) can be enforced in two different ways. One way is to enforce that the magnitude of the second-order tensor  $\bar{\boldsymbol{\sigma}}^{(2)}$  be zero, in which case there is a single *nonlinear* constraint, while a different, equivalent way is to enforce that each component of  $\bar{\boldsymbol{\sigma}}^{(2)}$  be zero, in which case there are several (three in the present case) *linear* constraints (see (30)). The latter approach has been found easier to implement and was therefore adopted in this work.

As already mentioned, of particular interest here are porous materials exhibiting *transversely isotropic* macroscopic response. In this connection, it should be noted that even if the matrix potential is isotropic, the effective potential (28)

is, in general, anisotropic. However, deBotton and Hariton [13] have shown, albeit numerically, that there are appropriate lamination sequences, i.e., particular choices of  $f_i$  and  $\mathbf{n}^{(i)}$ , for which the effective potential (28) tends to be transversely isotropic as the rank  $M$  increases. Motivated by those findings, the following lamination sequence has been adopted in this work:

$$f_i = \frac{1 - \frac{i}{M}(1-f)}{1 - \frac{i-1}{M}(1-f)} \tag{32}$$

$$\mathbf{n}^{(i)} = \cos \psi_i \mathbf{e}_1 + \sin \psi_i \mathbf{e}_2, \quad \psi_i = \frac{\eta}{2\pi} \frac{i-1}{M_\eta}, \quad i = 1, \dots, M \tag{33}$$

where  $f$  is the prescribed porosity in the rank- $M$  laminate, and the angles  $\psi_i$  determine the  $i$ th direction of lamination relative to the basis  $\{\mathbf{e}_i\}$ . In (33)<sub>2</sub>,  $\eta$  and  $M_\eta$  are two integers such that the rank of the laminate is  $M = \eta M_\eta$ . Thus, the set of angles  $\psi_i$  corresponds to  $M_\eta$  lamination directions (33)<sub>1</sub>, uniformly distributed on the unit circle, with  $\eta$  laminations for each direction. The potential (28) is insensitive to  $\eta$  in the linear case, but becomes more sensitive to this parameter with increasing nonlinearity. It has been verified numerically that, for this specific lamination sequence, the effective flow stress (28) becomes progressively less sensitive to the in-plane orientation of  $\bar{\sigma}$ , as the parameters  $M_\eta$  and  $\eta$  increase. The values  $\eta = 20$  and  $M_\eta = 50$ , which correspond to  $M = 1000$ , have been found adequate for the purposes of this work.

**4. Results and discussion**

In this section, the second-order estimates (*SOM*) proposed above for the effective behavior and the macroscopic strain-rates in transversely isotropic, power-law, porous materials, are compared with corresponding results generated by the sequential laminates (*LAM*) described in the previous section. In addition, these results are compared with the earlier ‘second-order’ (*SOMS*) estimates using the simpler prescription (21), as well as with the ‘variational’ estimates (*VAR*) and the Gurson [1] criterion (*GUR*) (for the case of ideally plastic materials). Note that Leblond et al. [3] only considered axisymmetric loadings for the cylindrical microstructures, and therefore it was not possible to compare with their estimates for power-law porous materials in this work. However, comparisons will be carried out elsewhere for the isotropic microstructures.

Fig. 1 shows the various estimates for the gauge function and the corresponding macroscopic triaxialities, for moderate values of the porosity ( $f = 10\%$ ) and nonlinearity ( $m = 1/n = 0.2$ ). The main observation in the context of this figure is that the *SOM* estimates proposed in this work are in very good agreement with the exact *LAM* results, for the entire range of macroscopic triaxialities. In contrast, the agreement exhibited by the *SOMS* estimates is very good for low triaxialities, but deteriorates for sufficiently large triaxialities.

In the hydrostatic limit, the *SOM* estimates coincide, by construction, with the exact result for *CCAs*, denoted by  $\square$  in Fig. 1(a). In turn, the *LAM* results, which correspond to high but finite rank laminates, also appear to tend to

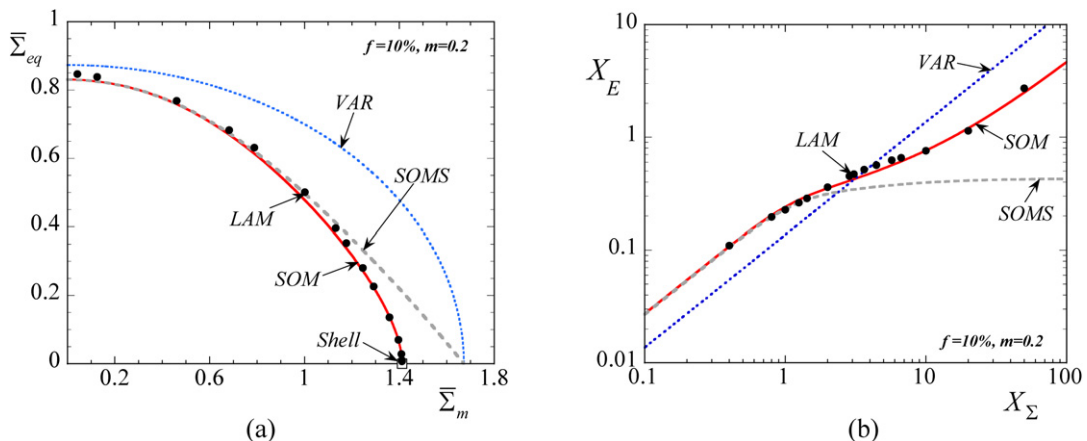


Fig. 1. (a) Gauge surfaces and (b) strain-rate – stress triaxiality plots for  $f = 10\%$  and  $m = 0.2$ .



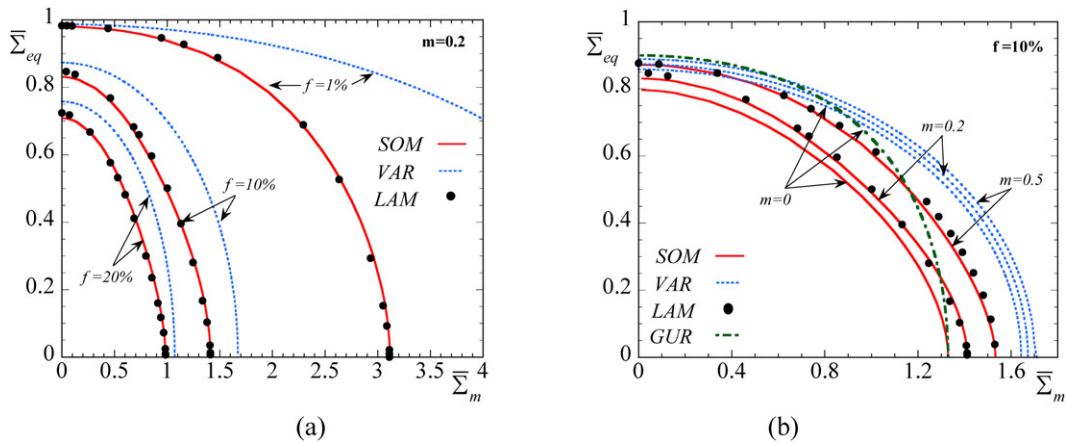


Fig. 2. Yield and gauge surfaces, as a function of (a) the porosity  $f$  and (b) the strain-rate sensitivity parameter  $m$ .

this exact result. Further support to the fact that the *LAM* results should agree exactly with the hydrostatic behavior of *CCAs* in the limit of infinite rank has been provided in [27]. On the other hand, both the *SOMS* curve (which corresponds to the choice (21) for the reference stress tensor), and the *VAR* estimates are seen to deviate from the analytical solution (19) in the hydrostatic limit. Note that Fig. 1(b) shows that, although the *VAR* prediction for the strain-rate triaxiality  $X_E$  tend to infinity as the stress triaxiality  $X_\Sigma$  becomes infinite, it deviates significantly from the *SOM* and the *LAM* estimates for the whole range of the stress triaxialities. On the other hand, the *SOMS* curve in this figure reaches an asymptotic value at high stress triaxialities (i.e.,  $\bar{D}_{eq} \neq 0$  as  $|X_\Sigma| \rightarrow \infty$ ), which is consistent with the existence of a corner in the  $\bar{\Sigma}_{eq}-\bar{\Sigma}_m$  plot. As already pointed out in Section 2, corners of this type have been observed by Pastor and Ponte Castañeda [10] for the case of ideal plasticity (i.e.,  $m = 0$ ), which may be caused by the development of shear bands in the matrix phase. However, it is unrealistic to expect formation of shear bands for a porous material whose matrix phase is described by an exponent  $m > 0$ . For this reason, we have assumed our new yield surfaces to be smooth on the hydrostatic axis (even in the ideally plastic limit).

Fig. 2 shows effective gauge surfaces,  $\Phi_n(\bar{\Sigma}_{eq}, \bar{\Sigma}_m) = 0$ , for different values of the porosity  $f$  and the strain-rate sensitivity parameter  $m$ . The gauge surfaces delivered by the *SOM* are in very good agreement with the *LAM* estimates for the whole range of  $\bar{\Sigma}_{eq}-\bar{\Sigma}_m$ . In particular, gauge surfaces are shown in Fig. 2(a) as functions of the porosity  $f$  for a given value of  $m = 0.2$ , where it is clearly observed that the *VAR* estimate significantly overestimates the resistance of the porous medium at high stress triaxialities and low porosities, when compared with the *SOM* and *LAM* estimates. However, it is worth noting that the estimate delivered by the *VAR* method in the hydrostatic limit improves at higher porosities (see corresponding curve for  $f = 20\%$  in Fig. 2(a)). This observation is a simple consequence of the fact that the *VAR* estimate (20) approaches the exact hydrostatic solution, given by relation (19), at high porosities.

Fig. 2(b) shows gauge surfaces as a function of the strain-rate sensitivity parameter  $m$  for a given value of porosity  $f = 10\%$ . Due to numerical difficulties, *LAM* results are only provided for  $m \geq 0.2$ . Similar to Fig. 2(a), the *SOM* and the *LAM* estimates are in very good agreement for the entire range of macroscopic triaxialities, while the *VAR* estimate, albeit a rigorous upper bound, remains too stiff as the nonlinearity of the matrix phase increases (i.e.,  $m$  decreases). In addition, for the special case of ideally plastic materials, the *GUR* estimate deviates significantly from the *SOM* estimate, despite the fact that it recovers the exact hydrostatic solution. As already anticipated, it violates the variational bound, *VAR*, for small stress triaxialities, in which case it tends to the Voigt bound. In any event, all the methods indicate a softening of the composite as the porosity or the nonlinearity increase, which is consistent with the contraction of the effective gauge surfaces.

In order to complete the study of the macroscopic properties of the porous composite, Fig. 3 shows the two ‘modes’ of the normalized, macroscopic strain-rate  $\bar{E}$ , the equivalent ( $\bar{E}_{eq}$ ) and the hydrostatic ( $\bar{E}_m$ ) mode, as functions of the strain-rate triaxiality  $X_E$  and the porosity  $f$ , for a fixed value of the nonlinearity  $m = 0.2$ . The estimates obtained by the *SOM* for the modes  $\bar{E}_{eq}$  and  $\bar{E}_m$  are found to be quite good, when compared with the *LAM* estimates, for the whole range of triaxialities and porosities, considered here. On the other hand, the *VAR* bound underestimates  $\bar{E}_{eq}$  at low triaxialities and  $\bar{E}_m$  at high triaxialities, when compared with the *LAM* and the *SOM* estimates. In particular,

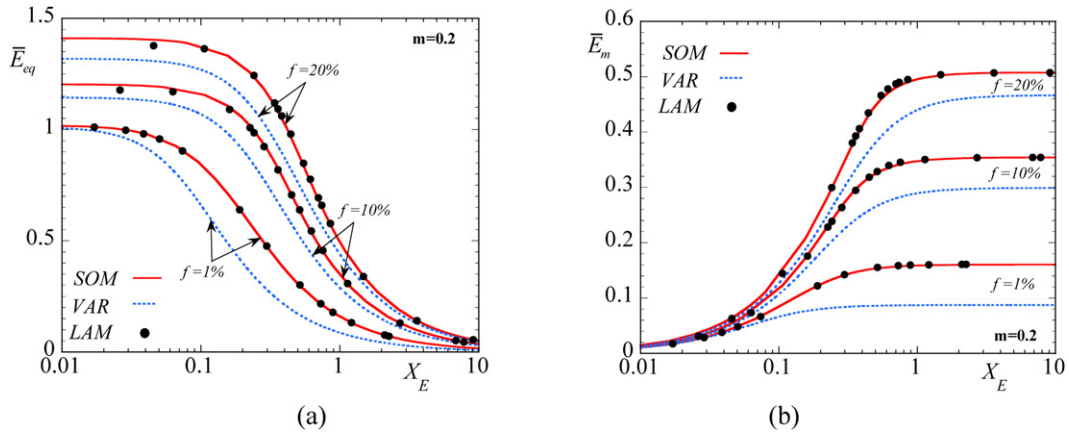


Fig. 3. Macroscopic strain-rates for  $m = 0.2$  as a function of the porosity  $f$  and the strain-rate triaxiality  $X_E$ . (a) shows the equivalent part  $\bar{E}_{eq}$  and (b) shows the hydrostatic part  $\bar{E}_m$  of the macroscopic strain-rate.

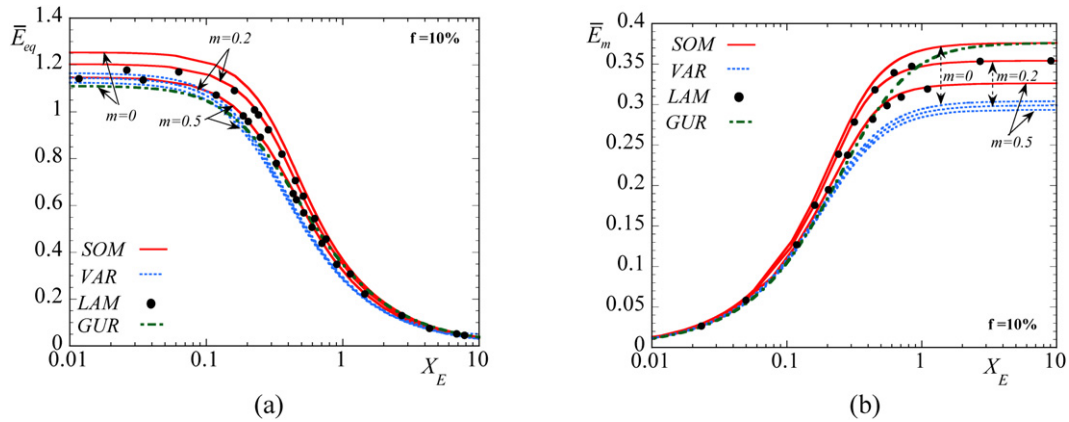


Fig. 4. Macroscopic strain-rates for  $f = 10\%$  as a function of the strain-rate sensitivity parameter  $m$  and the strain-rate triaxiality  $X_E$ . (a) shows the equivalent part  $\bar{E}_{eq}$  and (b) shows the hydrostatic part  $\bar{E}_m$  of the macroscopic strain-rate. The *SOM* estimates are compared with the *VAR* bound, the exact *LAM* results, and the *GUR* criterion.

at high triaxialities, it predicts an asymptotic value for  $\bar{E}_m$  that is 40% lower than the *SOM* estimate (see Fig. 3 for  $f = 1\%$ ), and thus than the exact result for  $\bar{E}_m$  obtained by direct derivation of the exact relation (19) with respect to  $\bar{\sigma}_m$ .

Finally, Fig. 4 shows  $\bar{E}_{eq}$  and  $\bar{E}_m$ , as functions of the strain-rate triaxiality  $X_E$  and the nonlinearity  $m$ , for a fixed value of the porosity  $f = 10\%$ . Note that for the case of  $m = 0$  (i.e., ideal plasticity) the *GUR* estimates are also shown. The *SOM* estimates are in very good agreement with the *LAM* results for the entire range of the strain-rate triaxiality and nonlinearities considered. On the other hand, as already anticipated, the *VAR* method underestimates the two modes  $\bar{E}_{eq}$  and  $\bar{E}_m$  at low and high strain-rate triaxialities, respectively. In addition, it is further noted that, although *GUR* recovers by construction the analytical estimate for  $\bar{E}_m$  and  $\bar{E}_{eq} = 0$  in the limit of hydrostatic loading for the case of ideally plastic materials (provided that the case of a corner in the yield surface is excluded), as shown in Fig. 4, it is found to underestimate both modes of the strain-rate for moderate to low triaxialities, when compared with the *SOM* estimates. It should be emphasized that the accurate prediction of  $\bar{E}_m$  is critical, as it controls the dilatation rate of the voids, which is even more sensitive at high triaxialities. The dilatation of the voids may lead to a significant increase of the porosity measure and eventually to the failure of the material. Therein lies the significance of the *GUR* model which was the first to be able to account for this effect.

### 5. Concluding remarks

In this work, a new model for transversely isotropic, porous media has been proposed. The new predictions were compared with exact *LAM* results and were found to be in excellent agreement for the whole range of triaxialities, porosities and nonlinearities considered. More specifically, the model is based on the ‘second-order’ nonlinear homogenization method, and makes use of a new prescription for the stress reference tensor, given by relation (22), which is such that the resulting second-order estimate reproduces exactly the in-plane hydrostatic behavior of the *CCA* microstructure.

The new estimates were found to improve significantly on earlier estimates, particularly at high triaxialities where both the variational method and the earlier versions of the second-order method had been found to significantly underestimate the hydrostatic part of the macroscopic average strain-rate, which is very important in the evolution of the porosity and failure of porous materials when subjected to high triaxial loads.

The encouraging results obtained in this work for two-dimensional microstructures, provide motivation to apply the same general ideas for more realistic three-dimensional microstructures, where it is expected that similarly accurate results will be obtained. In the context of these materials, it is also important to emphasize that the new model may be extended for arbitrary pore shapes, where the effective behavior of the porous material turns out to be anisotropic and thus the estimation of its overall response becomes a more challenging task.

### Acknowledgements

The work of K.D. was supported by the international fellowship “Gaspard-Monge” of École polytechnique, and partially by the scholarship for Hellenes of the Alexander S. Onassis Public Benefit Foundation. The work of M.I.I. and P.P.C. was supported by the US National Science Foundation through Grants CMS-02-01454 and OISE-02-31867.

### Appendix A. Definition of the reference coefficients

The coefficients introduced in relation (22) are given by

$$t = \frac{1 + X_{\Sigma}^4}{1 + 2t_1 X_{\Sigma}^2 + X_{\Sigma}^4}, \quad \text{with } t_1 = 10 \left( 1 - \left( \frac{\arctan\left(\frac{10^4 f^3}{\exp(-f)}\right)}{\pi/2} \right)^4 \right) \tag{A.1}$$

and

$$\beta = \frac{40m^2}{1 + 10m^2} \left( 1 - \left( \frac{\arctan\left(\frac{10^4 f^2}{\exp(-500f)}\right)}{\pi/2} \right)^6 \right) \tag{A.2}$$

It should be emphasized that the coefficient  $\beta$  becomes approximately zero for porosities larger than 1% and for very high nonlinearities (i.e.,  $m$  smaller than 0.05) and hence it could be neglected in these cases.

### Appendix B. Computation of the coefficients $\alpha_m$ and $\alpha_{eq}$ in ideal plasticity

In the special case of hydrostatic loading and rigid-perfectly plastic behavior ( $m = 0$ ), the equation (14) for the anisotropy ratio  $k$  simplifies significantly, which allows the analytical evaluation of the  $\alpha_m$  factor of the reference stress tensor (see relation (22)), which is given by

$$\alpha_m = \frac{3}{2} \frac{f(1 - k_H)^2 \sqrt{k_H}}{(1 - f)^2 (2k_H - 1)} \tag{B.1}$$

where

$$k_H = \frac{(3 + 2\sqrt{3}\sqrt{3 + 2g^2} \cos[\frac{1}{3} \arccos(\frac{-3\sqrt{3}(-1+g^2)}{\sqrt{(3+2g^2)^3}})])^2}{36g^2}, \quad \text{with } g = \frac{2(1 - f)^2}{f \ln(1/f)^2} \tag{B.2}$$

It is worth noting from relation (B.1), that  $k_H \geq \frac{1}{2}$ . The coefficient  $\alpha_{eq}$  may be further simplified in this case to

$$\alpha_{eq} = \frac{1}{\alpha_m} \frac{k_H - f}{1 - f} \tag{B.3}$$

## References

- [1] A.L. Gurson, Continuum theory of ductile rupture by void nucleation and growth, *J. Engrg. Mater. Technol.* 99 (1977) 2–15.
- [2] Z. Hashin, The elastic moduli of heterogeneous materials, *J. Appl. Mech.* (1962) 143–150.
- [3] J.B. Leblond, G. Perrin, P. Suquet, Exact results and approximate models for porous viscoplastic solids, *Int. J. Plasticity* 10 (1994) 213–235.
- [4] P. Ponte Castañeda, The effective mechanical properties of nonlinear isotropic composites, *J. Mech. Phys. Solids* 39 (1991) 45–71.
- [5] J.R. Willis, On methods for bounding the overall properties of nonlinear composites, *J. Mech. Phys. Solids* 39 (1991) 73–86.
- [6] J.C. Michel, P. Suquet, The constitutive law of nonlinear viscous and porous materials, *J. Mech. Phys. Solids* 40 (1992) (1991) 783–812.
- [7] Z. Hashin, S. Shtrikman, A variational approach to the theory of the elastic behavior of multiphase materials, *J. Mech. Phys. Solids* 11 (1963) 127–140.
- [8] P. Ponte Castañeda, Second-order homogenization estimates for nonlinear composites incorporating field fluctuations. I. Theory, *J. Mech. Phys. Solids* 50 (2002) 737–757.
- [9] P. Ponte Castañeda, Second-order homogenization estimates for nonlinear composites incorporating field fluctuations. II. Applications, *J. Mech. Phys. Solids* 50 (2002) 759–782.
- [10] J. Pastor, P. Ponte Castañeda, Yield criteria for porous media in plane strain: second-order estimates versus numerical results, *C. R. Mecanique* 330 (2002) 741–747.
- [11] J.F. Despois, R. Mueller, A. Mortensen, Uniaxial deformation of microcellular metals, *Acta Mater.* 54 (2006) 4129–4142.
- [12] G. deBotton, P. Ponte Castañeda, On the ductility of laminated materials, *Int. J. Solids Struct.* 29 (1992) 2329–2353.
- [13] G. deBotton, I. Hariton, High-rank nonlinear sequentially laminated composites and their possible tendency towards isotropic behavior, *J. Mech. Phys. Solids* 50 (2002) 2577–2595.
- [14] M.I. Idiart, Macroscopic behavior and field statistics in viscoplastic composites, Ph.D. thesis, University of Pennsylvania, 2006.
- [15] G. Francfort, F. Murat, Homogenization and optimal bounds in linear elasticity, *Arch. Rat. Mech. Anal.* 94 (1986) 307–334.
- [16] G.W. Milton, *The Theory of Composites*, Cambridge University Press, 2002.
- [17] R. Hill, Elastic properties of reinforced solids: some theoretical principles, *J. Mech. Phys. Solids A* 11 (1963) 127–140.
- [18] P. Ponte Castañeda, Exact second-order estimates for the effective mechanical properties of nonlinear composite materials, *J. Mech. Phys. Solids* 44 (1996) 827–862.
- [19] V.M. Levin, Thermal expansion coefficients of heterogeneous materials, *Mekh. Tverd. Tela* 2 (1967) 83–94.
- [20] J.R. Willis, Bounds and self-consistent estimates for the overall moduli of anisotropic composites, *J. Mech. Phys. Solids* 25 (1977) 185–202.
- [21] J.D. Eshelby, The determination of the elastic field of an ellipsoidal inclusion and related problems, *Proc. R. Soc. Lond. A* 241 (1957) 376–396.
- [22] M.I. Idiart, K. Danas, P. Ponte Castañeda, Second-order estimates for nonlinear composites and application to isotropic constituents, *C. R. Mecanique* 334 (2006) 575–581.
- [23] M.I. Idiart, P. Ponte Castañeda, Field statistics in nonlinear composites. I: Theory, *Proc. R. Soc. A* 463 (2007) 183–202.
- [24] M.I. Idiart, P. Ponte Castañeda, Second-order estimates for nonlinear isotropic composites with spherical pores and rigid particles, *C. R. Mecanique* 333 (2005) 147–154.
- [25] N. Bilger, F. Auslender, M. Bornert, J.-C. Michel, H. Moulinec, P. Suquet, A. Zaoui, Effect of a nonuniform distribution of voids on the plastic response of voided materials: a computational and statistical analysis, *Int. J. Solids Struct.* 29 (2005) 517–538.
- [26] P. Ponte Castañeda, Bounds and estimates for the properties of nonlinear heterogeneous systems, *Philos. Trans. Roy. Soc. London A* 340 (1992) 531–567.
- [27] M.I. Idiart, Nonlinear sequential laminates reproducing hollow sphere assemblages, *C. R. Mecanique* 335 (7) (2007) 363–368.